

PDF hosted at the Radboud Repository of the Radboud University Nijmegen

The following full text is a publisher's version.

For additional information about this publication click this link.

<http://hdl.handle.net/2066/28563>

Please be advised that this information was generated on 2018-07-07 and may be subject to change.



ELSEVIER

Surface Science 331–333 (1995) 1367–1371

surface science

Oxide-thickness dependence of second harmonic generation from thick thermal oxides on Si(111)

C.W. van Hasselt^a, E. Mateman^a, M.A.C. Devillers^a, Th. Rasing^{a,*},
A.A. Fedyanin^b, E.D. Mishina^b, O.A. Aktsipetrov^b, J.C. Jans^c

^a Research Institute for Materials, University of Nijmegen, Toernooiveld, NL 6525 ED Nijmegen, The Netherlands

^b Physics Department, Moscow State University, Moscow 119899, Russian Federation

^c Philips Research Laboratory, P.O. Box 80000, NL 5600 JA Eindhoven, The Netherlands

Received 20 September 1994; accepted for publication 22 November 1994

Abstract

We show here that the oxide-thickness dependence of the s-polarized SHG from Si(111) covered with a thick thermal oxide is completely described by multiple reflections in the oxide film. For the p-polarized response, a strong enhancement with thickness is observed, which cannot be explained in this way. These measurements show that one should be cautious in analyzing the SHG from a buried interface, and carefully take into account the linear optics involved.

Keywords: Crystalline–amorphous interfaces; Second harmonic generation; Semiconductor–insulator interfaces; Silicon; Silicon oxides

1. Introduction

Based on the symmetry breaking at an interface, optical second harmonic generation (SHG) from metal and semiconductor surfaces and interfaces has been developed as an extremely sensitive and versatile surface probe [1,2]. One of the most important advantages of this method is the possibility to use SHG to probe buried interfaces, such as the technologically important Si–SiO₂ interface. Recently a number of such experiments have been performed, showing the influence of interface strain [3,4], interface charge and electric field [5], preparation [6] and roughness [7]. Given the importance of the Si–SiO₂ interface, these various observations and interpreta-

tions call for a more systematic approach to the applicability of SHG as a diagnostic interface probe.

Recently we have shown that the strong thickness dependence of the s-polarized SHG under s-polarized excitation from thick thermal oxides on Si(111) can be totally explained by linear optics [8]. This was demonstrated in scans of both the angle of incidence and oxide thickness. To further study this problem we have measured the s- and p-polarized SHG response at the Brewster angle for the air–SiO₂ interface at 56° for the p-polarized fundamental beam, thereby excluding multiple reflections for ω . The oxide thicknesses ranged from 2 to 300 nm. We find that the changes in s-polarized SHG, both for s- and p-polarized input, as a function of oxide thickness and angle of incidence can be completely described by multiple reflections in the SiO₂ layer. The p-polarized SHG results for p-polarized excitation show

* Corresponding author.

E-mail: theoras@sci.kun.nl.

a strong thickness dependence that cannot be explained by linear effects.

2. Theory

For a Si(111)–SiO₂ surface, excited by a single pump field at frequency ω the surface and bulk contributions to the SHG response tensor $\chi^{(2)}$ cannot be separated in a single experiment [9,10]. The reflected s-polarized SHG intensity under s(p)-polarized excitation $I_{s,s}$ ($I_{p,s}$) is purely anisotropic and can be written as [8,10–12]

$$I_{s,s(p,s)}(2\omega) \sim |L_{2\omega} \chi^{(2)} L_{\omega}^2 \sin(3\psi)|^2 I^2(\omega). \quad (1)$$

Here ψ is the angle between the in-plane (11 $\bar{2}$) direction and the plane of incidence, I_{ω} is the pump intensity, L_{ω} and $L_{2\omega}$ are the linear Fresnel factors at ω and 2ω respectively and $\chi^{(2)}$ is the effective SHG response parameter.

The p-polarized SHG intensity under p-polarized excitation $I_{p,p}$ contains both isotropic and anisotropic contributions from a number of tensor elements, and can be written as [10–12]

$$I_{p,p}(2\omega) \sim \left| \sum_i L_{i,2\omega} \chi_i^{(2)} L_{i,\omega}^2 + \sum_i L_{i,2\omega} \chi_i^{(2)} L_{i,\omega}^2 \cos(3\psi) \right|^2 I^2(\omega). \quad (2)$$

Here the summation over i is over the isotropic and anisotropic contributions respectively, and $L_{i,\omega}$ and $L_{i,2\omega}$ are the corresponding linear Fresnel factors. We include SHG contributions from the silicon bulk, the Si–SiO₂ interface and a possible SiO_x or crystalline SiO₂ transition layer, i.e. all contributions that can be effectively described as coming from the interface region between Si and SiO₂. For a layer of SiO₂ on Si(111) no significant extra contributions to the nonlinear polarization at frequency 2ω are expected, because the SiO₂–air interface and the bulk SiO₂ have a very low nonlinear response (SiO₂ is centrosymmetric). This is in contrast to some recent observations that report a distinct effect of the oxide thickness on the SHG [4,13].

Although the oxide layer should not influence the nonlinear susceptibility, it can have a very strong effect on the linear optics involved, and therefore on

the total SHG intensity observed. Since the oxide layer has a refractive index between air and Si, and is transparent throughout a large part of the spectrum, multiple reflections for both ω and 2ω will play a role. We use the convention that the effective SHG source is located just below the Si–SiO₂ interface ($z = 0$), inside the silicon (which we define as $z = 0^-$). It should be stressed that this choice is not critical, since other choices only rescale the SHG response parameters in terms of an (interface) dielectric constant. To find the SHG intensity we first calculate the transmitted fundamental electric field E_t at the Si–SiO₂ interface:

$$E_t(z = 0^-) = t(z = 0^-) E_{in}, \quad (3)$$

where E_{in} is the incoming fundamental electric field in ambient, and t is the transmission through the SiO₂ and the Si, evaluated just below the Si–SiO₂ interface at $z = 0^-$ [14]. This means that the phase rotation upon reflection from the Si–SiO₂ interface is taken into account, but that the absorption inside the silicon does not play a role. The Fresnel factor L_{ω} is then given by

$$L_{\omega} = t(z = 0^-). \quad (4)$$

The wavevectors for the fundamental and SHG field are matched by the nonlinear boundary condition [15]:

$$k_{\parallel}(2\omega) = 2k_{\parallel}(\omega), \quad (5)$$

and the Fresnel factor $L_{2\omega}$ for the propagation of the SHG field into ambient is calculated in an analogous way. The interference in the oxide film is determined by the phase changes $\Phi_{i,j}$ upon reflection from the interface between medium i and j , and the phase change β due to the propagation through the oxide. For a nonabsorbing film like SiO₂ the $\Phi_{i,j}$ are constant and β is given by

$$\beta = \frac{2\pi}{\lambda_0} n d \cos \theta, \quad (6)$$

where λ_0 is the wavelength in ambient, n is the (real) refractive index, d the film thickness, and θ is the angle of propagation in the oxide film. From Eq. (6) it can immediately be seen that the Fresnel factors L_{ω} and $L_{2\omega}$ depend on the oxide thickness. Using these calculations we have shown that the strong oxide-thickness dependence for s-polarized

SHG under s-polarized excitation is completely described by multiple reflections [8]. Here, we will use this approach to calculate the SHG response for the other polarization combinations as well. To calculate SHG from arbitrary multilayer structures, this calculation of the Fresnel factors can more elegantly be written in a matrix formalism [16].

3. Experiment

The samples used were standard Si(111) ($\pm 0.5^\circ$) wafers. On these samples a high quality thermal oxide with a thickness of 300 nm was grown at 1000° . An annealing step at a slightly higher temperature in a nitrogen atmosphere was used to produce a smooth Si–SiO₂ interface. HRTEM images of this interface were made, showing that the Si–SiO₂ interface was atomically flat, with a corrugation of just two atomic layers over macroscopic distances ($\sim 100 \mu\text{m}$). A commercially available buffered NH₄F-etch solution with an etch-speed of $\sim 25 \text{ nm/min}$ was used to etch the SiO₂. In this way one sample was prepared in a 3×3 checkerboard configuration with nine different oxide thicknesses ranging from 2 to 151 nm. The other sample was prepared as a 5×5 checkerboard with 25 different oxide thicknesses ranging from 57 to 308 nm. The samples had some overlapping thicknesses. HRTEM pictures showed that the etching of SiO₂ did not influence the buried Si–SiO₂ interface, as is expected for a homogenous etching of a high-quality dense oxide layer. Extensive linear optical measurements were performed on these samples to characterize the optical constants and check the optical quality of the SiO₂ layer. Single-wavelength ellipsometry with a HeNe laser (632.8 nm) was used to measure all SiO₂ thicknesses prior to and after etching, and to check the homogeneity in thickness for a particular square on the checkerboard samples. Near-normal incidence reflectance spectroscopy between 200 and 1200 nm on the 5×5 sample validated the use of literature optical constants for Si [17] and SiO₂ [18], and the description of Si–SiO₂ in terms of a two-layer system with thickness-independent optical constants for SiO₂. As far as the linear optics is concerned there was no significant indication of a transition layer between Si and SiO₂ (like e.g. SiO_x or crystalline

SiO₂), in qualitative agreement with the HRTEM images.

The SHG experiments were performed in air using the frequency-doubled output at 532 nm of a seeded Q-switched Nd:YAG laser. The fluence of the 8 ns pulses was limited to 10 mJ in a 4 mm diameter spot, well below the damage threshold. The SHG signal was recorded using appropriate filters, a monochromator, photomultiplier and a gated integrator. For the 3×3 and 5×5 stepped oxides the amplitudes of $I_{p,s}$ and $I_{p,p}$ were measured as a function of the oxide thickness at the Brewster angle of 56° by translating the sample through the laser-beam.

4. Results and discussion

In Fig. 1, $I_{p,s}$ is plotted versus oxide layer thickness. The measurements were performed on both the 3×3 and the 5×5 samples at an angle of incidence of 56° , and matched at the overlapping thickness of 87 nm. As the input beam is very close to the Brewster angle for ω (55.6°), multiple reflections for ω are excluded. However, for the s-polarized 2ω beam the multiple reflections still play a role and must be taken into account. For this polarization combination only anisotropic signals are measured. If there are additional contributions to the SHG from

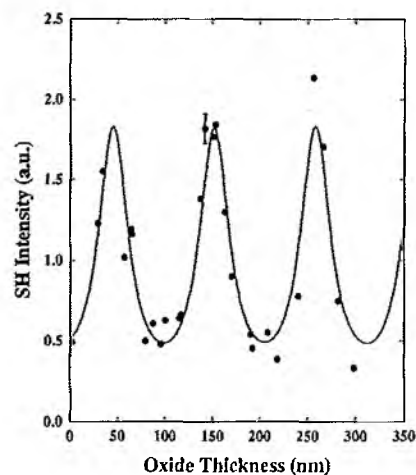


Fig. 1. Amplitude of $I_{p,s}$ as a function of oxide thickness at an angle of incidence of 56° . The solid line is the result of the model.

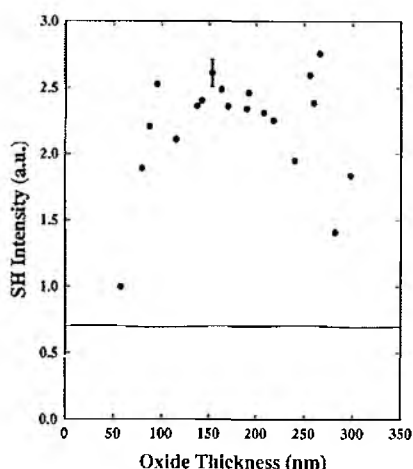


Fig. 2. Amplitude of $I_{p,p}$ as a function of oxide thickness at an angle of incidence of 56° . The solid line is the result of the model.

the SiO_2 itself, due to e.g. strain or a crystalline transition layer at the Si– SiO_2 interface, they are expected to be isotropic and so will not contribute to this polarization combination. The model is seen to describe the measurements very well, showing clear oscillations that are due to multiple reflections for 2ω . Note that the model does not contain any free parameters, other than an irrelevant scaling factor.

In Fig. 2, $I_{p,p}$ is plotted versus oxide layer thickness, measured on the 5×5 sample, at an angle of incidence of 56° (very close to the Brewster angle for both ω and 2ω at 55.6° and 56.3° respectively), thereby mostly excluding multiple reflections for both ω and 2ω . Also plotted is the theoretical thickness dependence as follows from our model. The measurement shows a very drastic oxide-thickness dependence, in contrast with the theoretical prediction. For p-polarized SHG under p-polarized excitation there are both isotropic and anisotropic contributions. These can then no longer be characterized by a single $\chi^{(2)}$ tensor element, as can be seen from Eq. (2). However, from Snell's law and the Fresnel formulae [14] it follows that for a nonabsorbing film (like the SiO_2) and for pure s- or p-polarized light the propagation direction and polarization of the transmitted and reflected light are independent of film thickness. In our case it means that, given the effective source for SHG at the Si– SiO_2 interface, the orientation of the electric fields at ω and 2ω

with respect to the crystal coordinate system are independent of oxide thickness. This, in turn means that all the Fresnel coefficients $L_{i,\omega}$ and $L_{i,2\omega}$ will depend on oxide thickness in the same way. So the amplitude of the p-polarized SHG anisotropy under p-polarized excitation $I_{p,p}$ as a function of oxide thickness should also be completely described by our multiple reflections model. Fig. 2 shows that this is absolutely not the case. In order to understand the origin of this strong thickness dependence of $I_{p,p}$, more theoretical work is in progress.

5. Conclusions

We have shown that the strong thickness dependence of the s-polarized SHG signal from thick thermal oxide layers on Si(111) is due to multiple reflections in this oxide layer. For this polarization we measure only the well-known anisotropic contribution from the Si– SiO_2 interface and the Si bulk. However, for the p-polarized SHG there is a very clear deviation from the multiple reflection model. This indicates that there are additional sources for SHG, or that there is a change in the present SHG response due to the SiO_2 layer, both of which should be oxide thickness dependent.

Acknowledgements

We would like to thank S. Bakker from Groningen University for the preparation of the thick thermal oxide samples and Dr. H. Zandbergen from the National Centre for High Resolution Electron Microscopy in Delft for making the HRTEM pictures. O.A.A., A.A.F. and E.D.M. would like to thank the RIM for their hospitality and financial support. Part of this work was supported by the Stichting voor Fundamenteel Onderzoek der Materie (FOM), which is financially supported by the Nederlandse Organisatie voor Wetenschappelijk Onderzoek (NWO).

References

- [1] T.F. Heinz, in: *Nonlinear Surface Electromagnetic Phenomena*, Eds. H.E. Ponath and G.I. Stegeman (North-Holland, Amsterdam, 1991) ch. 5.

- [2] Y.R. Shen, *Surf. Sci.* 299/300 (1994) 551.
- [3] W. Daum, H.J. Krause, U. Reichel and H. Ibach, *Phys. Rev. Lett.* 71 (1993) 1234.
- [4] S.V. Govorkov, N.I. Koroteev, G.I. Petrov, I.L. Shumay and V.V. Yakovlev, *Appl. Phys. A* 50 (1990) 439.
- [5] O.A. Aktsipetrov, L.M. Baranova, K.N. Evtyukhov, T.V. Murzina and I.V. Chernyi, *Sov. J. Quantum Electron.* 22 (1992) 807.
- [6] C.H. Bjorkman, C.E. Shearon, Y. Ma, T. Yasuda, G. Lucovsky, U. Emmerichs, C. Meyer, K. Leo and H. Kurz, *J. Vac. Sci. Technol. A* 11 (1993) 964; *J. Vac. Sci. Technol. B* 11 (1993) 1521.
- [7] J.I. Dadap, B. Doris, Q. Deny, M.C. Downer, J.K. Lowell and A.C. Diebold, *Appl. Phys. Lett.* 64 (1994) 2139.
- [8] C.W. van Hasselt, M.A.C. Devillers, Th. Rasing and O.A. Aktsipetrov, *J. Opt. Soc. Am. B* 12 (1995) 33.
- [9] R.W.J. Hollering, *J. Opt. Soc. Am. B* 8 (1991) 374.
- [10] J.E. Sipe, D.J. Moss and H.M. van Driel, *Phys. Rev. B* 35 (1987) 1129.
- [11] H.W.K. Tom, T.F. Heinz and Y.R. Shen, *Phys. Rev. Lett.* 51 (1983) 1983.
- [12] O.A. Aktsipetrov, I.M. Baranova and Yu.A. Il'inskii, *Sov. Phys. JETP* 64 (1986) 167.
- [13] U. Emmerichs, C. Meyer, K. Leo, H. Kurz, C.H. Bjorkman, C.E. Shearon, Y. Ma, T. Yasuda and G. Lucovsky, *Mater. Res. Sci. Symp. Proc.* 281 (1992) 815.
- [14] M. Born and E. Wolf, *Principles of Optics* (Pergamon, Oxford, 1980).
- [15] Y.R. Shen, *The Principles of Nonlinear Optics* (Wiley, New York, 1984).
- [16] H.A. Wierenga, M.W.J. Prins and Th. Rasing, *Physica B* 204 (1995) 281.
- [17] D.E. Aspnes and A.A. Studna, *Phys. Rev. B* 27 (1983) 985.
- [18] E.D. Palik, Ed., *Handbook of Optical Constants of Solids* (Academic Press, New York, 1985).